2015

Evaluating a satellite-based seasonal evapotranspiration product and identifying its relationship with other satellite-derived products and crop yield: A case study for Ethiopia

Tsegaye Tadesse
University of Nebraska-Lincoln, ttadesse2@unl.edu

Gabriel B. Senay
USGS EROS, senay@usgs.gov

Getachew Berhan
Addis Ababa University

Teshome Regassa
University of Nebraska-Lincoln, tregassa2@unl.edu

Shimelis Beyene
University of Nebraska-Lincoln

International Journal of Applied Earth Observation and Geoinformation 40 (2015) 39–54

Contents lists available at ScienceDirect

International Journal of Applied Earth Observation and Geoinformation

journal homepage: www.elsevier.com/locate/jag

Evaluating a satellite-based seasonal evapotranspiration product and identifying its relationship with other satellite-derived products and crop yield: A case study for Ethiopia

Tsegaye Tadesse[a,*], Gabriel B. Senay[b], Getachew Berhan[c], Teshome Regassa[d], Shimelis Beyene[e]

[a] National Drought Mitigation Center, School of Natural Resources, University of Nebraska-Lincoln, 816 Hardin Hall, 3310 Holdrege Street, P.O. Box 830988, Lincoln, NE 68583-0988, USA
[b] U.S. Geological Survey (USGS) Earth Resources Observation and Science (EROS) Center, 47914 252nd Street, Sioux Falls, SD 57198, USA
[c] Addis Ababa University, P.O. Box 1176, Addis Ababa, Ethiopia
[d] Department of Agronomy and Horticulture, University of Nebraska-Lincoln, USA
[e] Institute for Ethnic Studies, Department of Anthropology, University of Nebraska-Lincoln, USA

ARTICLE INFO

Article history:
Received 19 July 2014
Accepted 13 March 2015

Keywords:
Crop yield
Drought
Early warning
Evapotranspiration
Food security
Risk management

ABSTRACT

Satellite-derived evapotranspiration anomalies and normalized difference vegetation index (NDVI) products from Moderate Resolution Imaging Spectroradiometer (MODIS) data are currently used for African agricultural drought monitoring and food security status assessment. In this study, a process to evaluate satellite-derived evapotranspiration (ETa) products with a geospatial statistical exploratory technique that uses NDVI, satellite-derived rainfall estimate (RFE), and crop yield data has been developed. The main goal of this study was to evaluate the ETa using the NDVI and RFE, and identify a relationship between the ETa and Ethiopia's cereal crop (i.e., teff, sorghum, corn/maize, barley, and wheat) yields during the main rainy season. Since crop production is one of the main factors affecting food security, the evaluation of remote sensing-based seasonal ETa was done to identify the appropriateness of this tool as a proxy for monitoring vegetation condition in drought vulnerable and food insecure areas to support decision makers. The results of this study showed that the comparison between seasonal ETa and RFE produced strong correlation ($R^2 > 0.99$) for all 41 crop growing zones in Ethiopia. The results of the spatial regression analyses of seasonal ETa and NDVI using Ordinary Least Squares and Geographically Weighted Regression showed relatively weak yearly spatial relationships ($R^2 < 0.7$) for all cropping zones. However, for each individual crop zones, the correlation between NDVI and ETa ranged between 0.3 and 0.84 for about 44% of the cropping zones. Similarly, for each individual crop zones, the correlation (R^2) between the seasonal ETa anomaly and de-trended cereal crop yield was between 0.4 and 0.82 for 76% (31 out of 41) of the crop growing zones. The preliminary results indicated that the ETa products have a good predictive potential for these 31 identified zones in Ethiopia. Decision makers may potentially use ETa products for monitoring cereal crop yields and early warning of food insecurity during drought years for these identified zones.

1. Introduction

Recent studies have shown the importance of remotely sensed data in improving drought and vegetation monitoring for risk management (Tadesse et al., 2014; Rojas et al., 2011; Mishra and Singh, 2011; Meze-Hausken, 2004). Given the repeat coverage and spatially continuous measurements over a large area, satellite-based remote sensing plays a vital role in monitoring drought on a more local scale. In addition, advanced satellite technology products with high temporal resolution are cost effective and may serve to detect the onset of a drought and its duration and magnitude, which is critical information for risk management and food security. Monitoring crop production to provide early warning of production shortfalls during extreme climate events such as drought is a key objective of many governments. Thus, satellite information and

* Corresponding author. Tel.: +1 402 472 3383.
E-mail addresses: ttadesse2@unl.edu (T. Tadesse), senay@usgs.gov (G.B. Senay), getachewb1@yahoo.com (G. Berhan), tregassa2@unl.edu (T. Regassa), sbeyene2@unl.edu (S. Beyene).

http://dx.doi.org/10.1016/j.jag.2015.03.006

products are expected to help in decision making for countries with a wide diversity of crops, ecosystems, and production systems.

Food production and water scarcity are long-standing issues in Ethiopia, exacerbated by periodic drought and an ever-increasing population (Tadesse et al., 2014; Meze-Hausken, 2004). Agriculture continues to be a predominant sector of the economy and an important sector that provides food to the fast-growing population. Generally, food insecurity typically results from a combination of climate events and societal vulnerabilities. In rainfed agriculture, availability of water is the most critical factor for sustaining crop productivity and food security. Recent droughts have illustrated the need for improved monitoring and enhanced decision support systems to deliver timely and reliable information products to decision makers at many levels (Tadesse et al., 2008). Several methods and approaches for drought monitoring and risk management have been developed in the last few decades (Tadesse et al., 2008; Panu and Sharmat, 2002). However, there is still an increasing demand to improve, test, and integrate existing satellite-derived products using integrated remote sensing and ground observation of climate data to address food production issues that arise from water scarcity and drought (Vicente-Serrano et al., 2012; Rojas et al., 2011; Mishra and Singh, 2011). In addition, the development of new tools that provide timely, detailed spatial-resolution drought information is essential for improving drought preparedness and response (Brown et al., 2008). Recent state-of-the-art drought monitoring tools, such as the vegetation drought response index (VegDRI) (Brown et al., 2008), Vegetation Outlook (VegOut) (Tadesse et al., 2010), and Atmosphere-Land Exchange Inverse (ALEXI) (Anderson et al., 2007) were developed to address vegetation stress using satellite and remote sensing data. Among these, drought and vegetation monitoring tools, only a few (e.g., ALEXI) are focused on the use of evapotranspiration (ET) data as a proxy for vegetation condition monitoring.

Bastiaanssen et al. (2005) and Senay et al. (2011) indicated that ET's dependence on land cover and soil moisture, and its direct relationship with carbon dioxide assimilation in plants, makes it an important variable to monitor and estimate crop yield and biomass for decision makers interested in food security. ET is the combined process of water surface evaporation, soil moisture evaporation, and plant transpiration. In the environmental system, ET is an important and primary component of the hydrologic budget because it expresses the exchange of mass and energy between the soil–water–vegetation system and the atmosphere. ET comprises two sub-processes: evaporation and transpiration. Evaporation occurs on the surfaces of open water bodies, vegetation, and bare ground. Transpiration involves the withdrawal and transport of water from the soil/aquifer system through plant roots, stems, and eventually an evaporation process from the interior of the plant leaves into the atmosphere (Senay et al., 2007, 2011). Prevailing weather conditions influence potential and reference ET through forcing variables such as radiation, temperature, wind, and relative humidity (Senay et al., 2011).

Since 2000, actual ET (ETa) data from the Moderate Resolution Imaging Spectroradiometer (MODIS) have been produced by the U.S. Geological Survey (USGS) Famine Early Warning Systems Network (FEWSNET) using the operational simplified surface energy balance (SSEBop) model (Senay et al., 2013). The SSEBop setup is based on the simplified surface energy balance (SSEB) approach (Senay et al., 2007, 2011) with unique parameterization for operational applications. The ETa may be used to show the current vegetation condition as compared to the long historical records. This comparison has the potential to help identify vegetation stress in time and space (Senay et al., 2013). For example, the ETa anomaly for a given period expresses the surplus or deficit of ETa as compared to the same period historically. FEWSNET (2014) noted that knowledge of the rate and amount of ETa for a given location is an essential component in the design, development, and monitoring of agricultural and environmental systems. Across the crop or rangeland areas, ETa anomalies are assumed to show (i) surplus or deficit in soil moisture during the non-growing season and (ii) surplus or deficit of crop water use in the growing season, which is directly related to crop condition and biomass. Thus, positive ETa anomalies expected to indicate relatively higher biomass, and negative ETa anomalies show less biomass as compared to the long historical record (median value) for the same period. Based on this assumption, ETa products are used for 8-day cumulative, monthly, and seasonal ET anomalies for Africa to monitor agricultural drought and food security status assessment (FEWSNET, 2014).

Despite the general consensus in using ETa anomalies for drought monitoring and food security assessment, a comprehensive model evaluation has not yet been done. Moreover, methodologies for evaluating drought and food security models are limited. Taking these gaps into account, this research has focused on developing a model evaluation method specifically applicable to drought and food security models using crop yield data. The specific objectives are to (1) develop a process to evaluate satellite-derived evapotranspiration anomalies using satellite-derived rainfall estimate (RFE), normalized difference vegetation index (NDVI), and crop yield data, (2) evaluate the potential use of ETa products in estimating the main cereal crops during the long rainy season (Kiremt) using the correlation between seasonal ETa anomaly and crop yield anomaly data, and (3) identify crop growing zones in Ethiopia that could potentially use the ETa products for monitoring crop yields to support risk management and food security.

2. Materials and methods

2.1. Study area selection for model evaluation

Ethiopia occupies a total area of 1,100,000 km^2 and is divided into 72 administrative zones (Fig. 1). The areas of these zones range from about 300 km^2 (Hareri zone) to 45,000 km^2 (Bale zone) (GeoHive, 2014). The average area of all zones is about 15,000 km^2. The global land cover map produced by the European Space Agency (ESA) was used to identify the cropland zones in Ethiopia. The ESA's global land cover map (GlobCover LC v2) is based on Medium Resolution Image Spectrometer (MERIS) sensor data with a spatial resolution of 300 meters (ESA, 2008). The geographic distribution of the cropland in Ethiopia and the crop growing zones are shown in Fig. 1. For this study, 41 crop growing zones that have about eleven years of historical records of yield data (2000–2010) were selected (Fig. 1).

2.2. The crop growing seasons and estimating crop yield in Ethiopia

The two main rainy seasons in Ethiopia are locally known as Kiremt (June–September) and Belg (February–May) (Diro et al., 2008; Gissila et al., 2004). Kiremt is the main rainy season across most parts of Ethiopia, except the extreme south and southeast part of the country (Gissila et al., 2004). The onset and withdrawal as well as the amount and distribution of precipitation during Kiremt have a greater impact on crop production than Belg (Evangelista et al., 2013). In addition, the Kiremt season yield accounts for 90–95% of the annual crop production of Ethiopia (Seifu, 2004; FEWSNET, 2003). Thus, this study focused on a crop yield anomaly for the Kiremt growing season.

Cereals are the major food crops in terms of area planted and volume of production in the selected zones (CSA, 2014). Cereals are also produced in greater volumes compared with other crops because they are the principal staple crops in these zones. The CSA

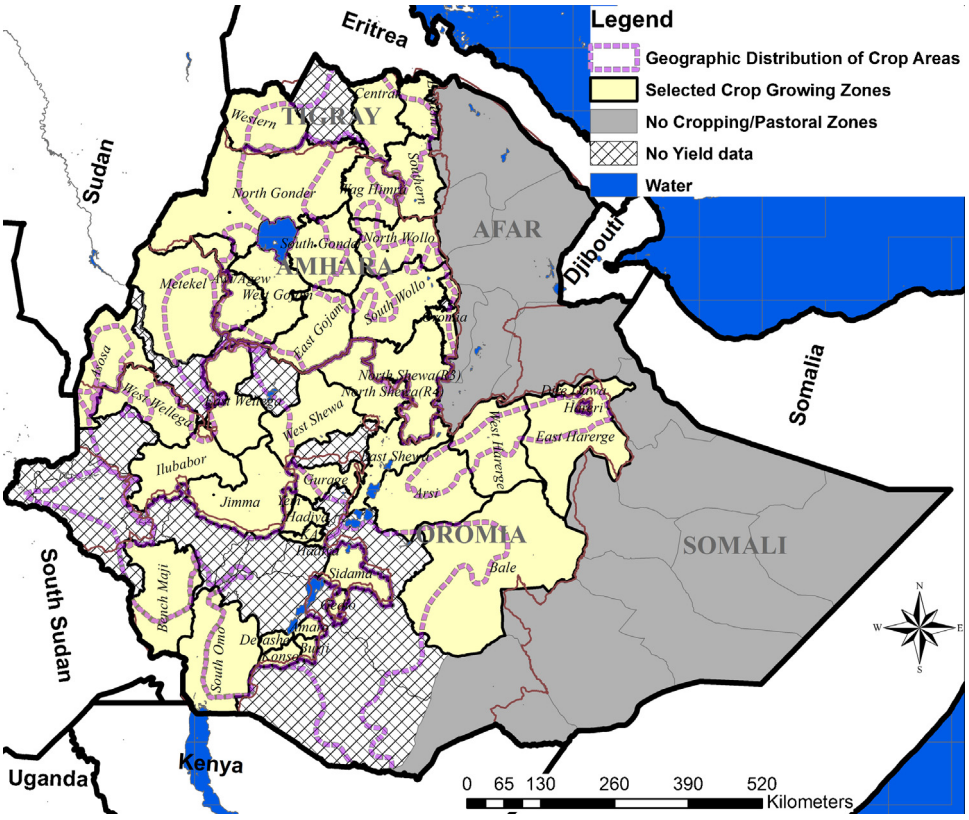

Fig. 1. Selected crop growing zones (yellow color on the map) of Ethiopia. (For interpretation of the references to colour in this figure legend, the reader is referred to the web version of this article.)

(2014) maintains crop yield data including cereals at the zonal (district) administrative level (about 15,000 km^2) in Ethiopia. For each zonal administrative area, the CSA uses standard statistical data collection and analysis to generate the estimate of the crop yield. In this process, to select a sample, a stratified two-stage cluster sample design is used. According to CSA (2014), the primary sampling units are enumeration areas and the secondary sampling units are agricultural households. An enumeration area in the rural parts of Ethiopia is a locality that consists, in most cases, of less than 150–200 households. A household may be either one person or multi-person. The enumeration areas from each stratum are selected systematically (using probability) in proportion to the size of agricultural households. The data collected using the standard CSA procedures are then entered into a database. These crop yield estimates at the zonal level are reported in the CSA yearly report (CSA, 2014).

Thus, over the 41 selected crop zones (Fig. 1), the cereal yield data were used for identifying possible relationships with ETa and assessing its potential use. The historical crop yield data from 2000 to 2010 were obtained from CSA. However, two years of data (2002 and 2009) were missing in CSA crop yield historical data reports. Thus, 2002 and 2009 were excluded in all correlation analysis in this study.

2.3. Preparing crop yield data for model evaluation

Data from analysis of the temporal and spatial variation of crop yield should be used to evaluate the model. According to FAO (1999), the factors that affect the temporal variability of agricultural yields can be generally grouped into three categories: (i) technology and management trends such as mechanization, varieties, irrigation, and the farmers' know-how, (ii) intermittent extreme factors of various origins and policy changes that affect management decisions (e.g., farmers' decisions to use less fertilizer if the policy is changed to no longer subsidize it), and (iii) pseudo-cyclic patterns such as weather that vary through time. Fig. 2 illustrates these factors.

In this study, the seasonal ETa anomaly evaluation is focused mainly on the effect of weather on crop yield data. However, it is often difficult to separate weather from other factors. One approach is to remove the trend that is assumed to be caused by factors other than weather (Wu et al., 2007). This practise is called detrending; it involves removing trends from regularly sampled time-domain input-output data (FAO, 1999). This data processing operation helps to estimate more accurate linear models because linear models cannot capture arbitrary differences between the input and output signal levels. It is also assumed that removing a trend from the data enables researchers to focus the analysis on the yearly variations in the crop yield data. Therefore, the crop yield data were first detrended before testing the correlation between ETa and crop yield data.

To eliminate the upward linear trend in a time series of yields due to several factors including advancements in agricultural technology and crop hybrids, the crop yield data were detrended by regression analysis of the annual zonal yields against the year. Ten years of historical crop yield data (2000–2010) from CSA were used to detrend the zonal yield statistics. To detrend annual crop yield, a linear trend equation (Eq. (1)) was used.

$$Y(t) = \alpha + \beta X(t) \quad (1)$$

where $Y(t)$ is the projected value of the crop yield for a specific year, α is the y-intercept (the estimated value of the crop yield at time $t=0$ or first year record), β is the slope of the trend line (or the average change in crop yield per year), and $X(t)$ is the year that the yield is estimated.

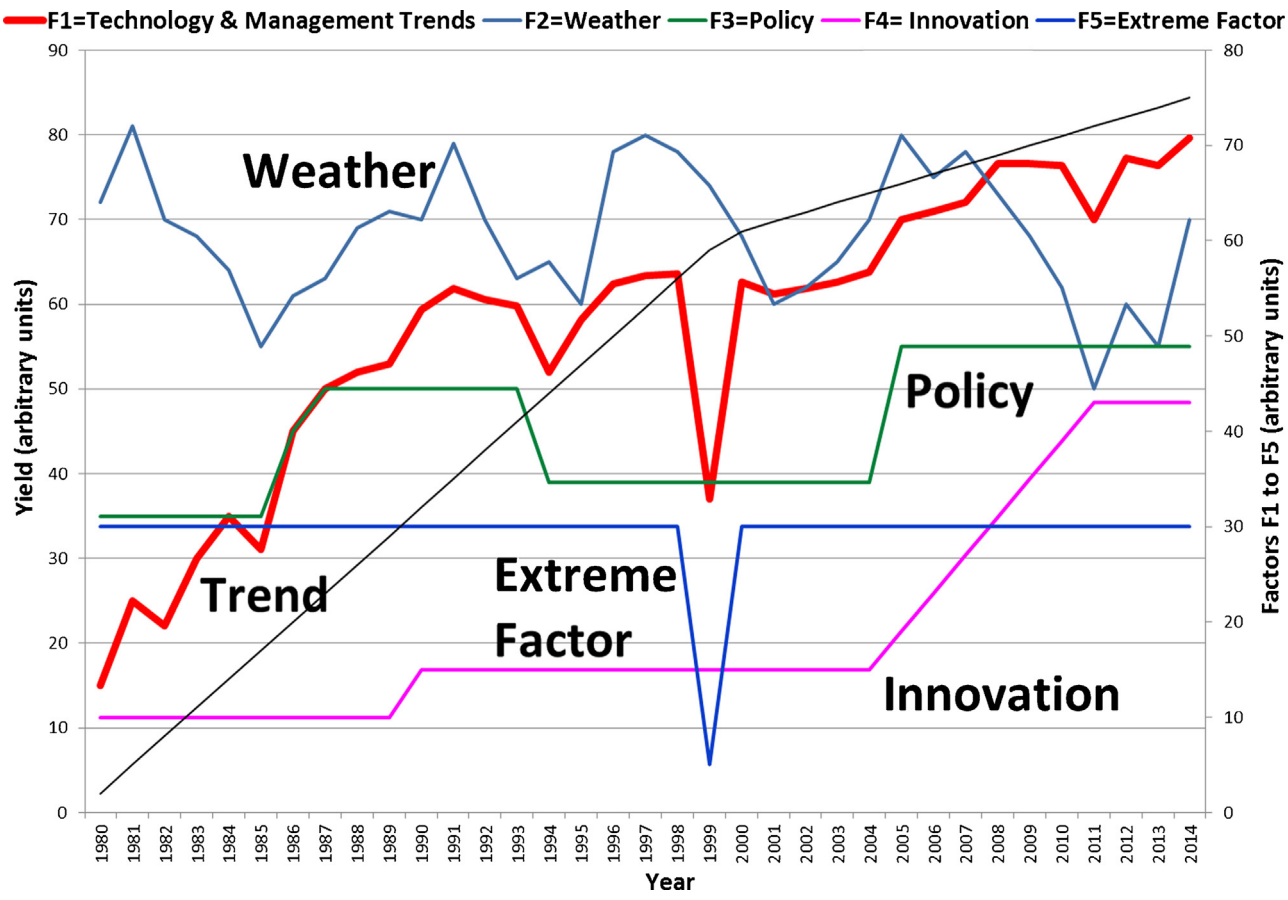

Fig. 2. Factors affecting agricultural yields: technology and management trends (heavy red line), innovation, policy, extreme factors, and weather (adapted from FAO, 1999). (For interpretation of the references to colour in this figure legend, the reader is referred to the web version of this article.)

After identifying the trend (using Eq. (1)) and generating the estimated values, detrending simply involves subtracting the estimated trend value from the actual crop yield data value for each given year. Matlab software was used to detrend the crop yield (MathWorks, 2009).

2.4. ETa model description

The ETa estimation methods can be grouped into two broad classes: (1) water balance and (2) energy balance. The water balance approach mainly considers the amount and temporal distribution of rainfall in meeting the crop water demand (ideal ET) through soil moisture modeling. The energy balance approach is driven by land surface temperature (LST) and is a more direct observation of the amount of water evapotranspired by the crop. The basic principle is that healthy and well-watered vegetation (and, consequently, freely transpiring vegetation) has a much cooler LST than unhealthy and water-stressed vegetation (Senay et al., 2013). An advantage of an energy balance model is that there is no need for prior knowledge of the crop calendar (e.g., crop type, start-of-season, and length of growing period), nor for assumptions on optimum management of the crop, as is the case for a water balance model (Senay et al., 2013). The LST provides an integrated parameter that takes into account the impact of water, disease, pests, management practises, and other factors on crop condition (as measured by ETa).

Most energy balance models, including the ETa estimation, require solving the energy balance equation expressed as:

$$LE = Rn - G - H \quad (2)$$

where LE = latent heat flux (energy consumed by evapotranspiration) (W/m^2); Rn = net radiation at the surface (W/m^2); G = ground heat flux (W/m^2); H = sensible heat flux (W/m^2).

At the land surface, the latent heat flux (comparable to ETa) is calculated as the residual of the difference between the net radiation to the surface and losses due to the sensible heat flux (energy used to heat the air) and ground heat flux (energy stored in the surface).

The ETa data used in this study were produced by the SSEBop model (SSEBop: FEWSNET, 2014) that directly solves for ET without explicitly estimating the other energy balance terms. The SSEBop ETa algorithm is an operational parameterization of the SSEB model (Senay et al., 2007), renamed as SSEBop (Senay et al., 2013). This approach assumes, for a given day and location, the temperature discontinuity between a bare-dry surface and atmosphere (dT) remains nearly constant from year-to-year under clear-sky conditions required for satellite observations, and that most of the surface energy balance is driven by the available clear-sky net radiation (Rn). This simplification permits the estimation of ET fraction as:

$$ETf = \frac{Th - Ts}{dT} \quad (3)$$

where ETf is the ET fraction (0–1); dT is a pre-defined (from clear-sky radiation balance calculation) temperature difference between the hot and cold reference boundary conditions that are unique for each day and pixel, ranging generally between 5 and 25 degree K depending on location and season. Th is the hot reference boundary condition, representing the temperature of a dry-bare (hot) surface (Th = Tc + dT); Tc is the cold boundary condition, representing the cold/wet-vegetated surface, which is in equilibrium with the air

temperature, i.e., all net radiation is used for latent heat flux. Tc is derived as fraction of the maximum air temperature (obtained from gridded weather fields); Ts is the surface temperature, derived from MODIS LST.

Actual ET is then estimated for a period of aggregation defined by the reference ("potential" ET, ETo), which is calculated from solving the Penman–Monteith equation (Allen et al., 2007; Senay et al., 2008) using weather parameters derived from model-assimilated global fields (Kanamitsu, 1989; Allen et al., 2007). Eight-day ETa estimates are then aggregated to monthly and seasonal totals.

$$ETa = ETf \times ETo \quad (4)$$

The ETa anomaly for a season in percent then is calculated as:

$$ETa\,(\%) = \frac{ETac}{ETam} \times 100 \quad (5)$$

where ET*a*(%) is anomaly percentage value, ETac is current seasonal ETa value and ETam is median value of ETa from 2000 to 2013 for the same season. This ETa anomaly for a given period is expected to show the surplus or deficit of ETa as compared to the same period historically. During the non-vegetative stage (for crop or rangeland areas), ETa anomalies are an expression of surplus or deficit in soil moisture. During the growing season, ETa anomalies express surplus or deficit crop water use, which is directly related to crop condition and biomass. Thus, positive ETa anomalies indicate greater-than-normal biomass (compared to the median value for the same period), and negative ETa anomalies indicate less-than-normal biomass (compared to the median value for the same period).

This method has been used over a 14-year MODIS history over the Conterminous United States (CONUS), Africa, and Southeast Asia, and has been validated comprehensively by Velpuri et al. (2013) against flux tower observations, water balance ET and MOD16 (Mu et al., 2007, 2011). More recently, Bastiaanssen et al. (2014) applied the SSEBop ET successfully in the Nile Basin for mapping water production and consumptions zones. However, the accuracy of the ET derived from the SSEBop model may vary from place to place depending on the accuracy of input parameters including weather data. In addition to the limitations of the model in complex terrain, the ET anomaly products may be useful for drought monitoring because the temporal variability is mainly driven by the LST and model errors are minimized (Senay et al., 2013).

2.5. Zonal statistics extraction for ETa

The available long historical records of seasonal (May–December) ETa data from 2000 to 2013 were used to extract the values at the zonal administrative level using an ArcGIS zonal statistics tool (ESRI, 2014). The crop layer based on the land cover map (GlobCover LC v2) was used to extract the zonal statistics. This was designed to analyze the cropping zones distinctly (i.e., differentiating from other land cover). Using the zonal map layer of Ethiopia, the seasonal ETa values within each zone were calculated. For ETa model evaluation, the mean values of seasonal ETa within each zone for all years were calculated for further correlation analysis. Thus, a database was built that includes all historical values of ETa (using zonal statistical mean) for all selected zones for 2000–2013.

2.6. Satellite-derived seasonal rainfall estimate data for ETa comparison

The RFE data are increasingly being used for many applications such as food security decisions in place of rainfall products based on gauge observations, or to supplement ground rainfall observations (Dinku et al., 2007; Joyce et al., 2004). Many satellite estimates have reasonable accuracy and good temporal and spatial resolutions (Dinku et al., 2014; Huffman et al., 2007). In this study, the RFE seasonal data (RFE version 2.0) that have been operational since 2001 by NOAA's Climate Prediction Center (CPC) (NOAA, 2014) were used. These CPC/Famine Early Warning System (FEWS) operational rainfall estimates include daily gridded data for Africa based on four sources: (i) Daily Global Telecommunication System rain gauge reports for up to 1000 stations, (ii) NOAA's Advanced Microwave Sounding Unit microwave satellite precipitation estimates up to 4 times per day, (iii) NOAA's Special Sensor Microwave/Imager (SSM/I) satellite rainfall estimates up to 4 times per day, and (iv) Geostationary Operational Environmental Satellite system (GEOS) Precipitation Index cloud-top infrared temperature precipitation estimates on a half-hour basis. The three satellite estimates are first combined linearly using predetermined weighting coefficients, then are merged with station data to determine the final African rainfall. The gridded RFE for Africa has 8 km resolution at a 10-day (decadal) time step. The ETa seasonal data were compared with the RFE seasonal data to identify their correspondence and relationships in Kiremt season. For this comparison, the dekadal RFE data were extracted for Ethiopia from 2000 to 2013 and then aggregated to a season (May–October). Then, based on this aggregated seasonal data, percent average precipitation was calculated for each year (i.e., current year seasonal total precipitation divided by seasonal precipitation mean of historical records, and then multiplied by 100). These percent average seasonal precipitation estimates were extracted for the selected cropping zones of Ethiopia to be compared with the seasonal ETa anomaly.

2.7. MODIS-based normalized difference vegetation index (NDVI) for ETa comparison

The NDVI is a measure of the density of chlorophyll contained in vegetative cover and is defined as (NIR - RED)/(NIR + RED), where NIR is the near-infrared reflectance and RED is the visible-red reflectance (Tucker et al., 1985). The NDVI is used to monitor vegetation condition in many parts of the world, including Africa (Tucker et al., 1985; Malingreau, 1986; Townshend et al., 1987; Reed et al., 1996; Myneni et al., 1997; Jakubauskas et al., 2002; DeBeurs and Henebry, 2004). In this study, the NDVI is calculated based on MODIS 10-day (dekad) maximum-value composite NDVI images at 250 m spatial resolution. This vegetation product is calculated from MODIS L1B Terra surface reflectance, corrected for molecular scattering, ozone absorption, and aerosols using MODIS Science Team algorithms (USGS, 2014). The NDVI data are temporally smoothed using a time series smoothing technique developed by Swets et al. (1999). This technique uses a weighted least squares linear regression approach to "correct" observations that are of poor quality because of clouds or other atmospheric contamination. In this study, these smoothed 10-day (decadal) time series NDVI data from May to December were aggregated to calculate the seasonal percent average NDVI values for each year from 2001 to 2013. Then, the seasonal average NDVI data were extracted for the selected cropping zones in Ethiopia to compare with the seasonal ETa anomaly for identifying the relationships and assessing their correspondence.

2.8. Spatial regression analysis of ETa, RFE, NDVI, and crop yield data

Because ETa, RFE, and NDVI have spatial dimensions, the relationships between these variables were determined using ordinary least square (OLS) and geographically weighted regression (GWR). The OLS is one of the best-known regression techniques to perform spatial regression analyses (Lloyd, 2007; Fotheringham et al.,

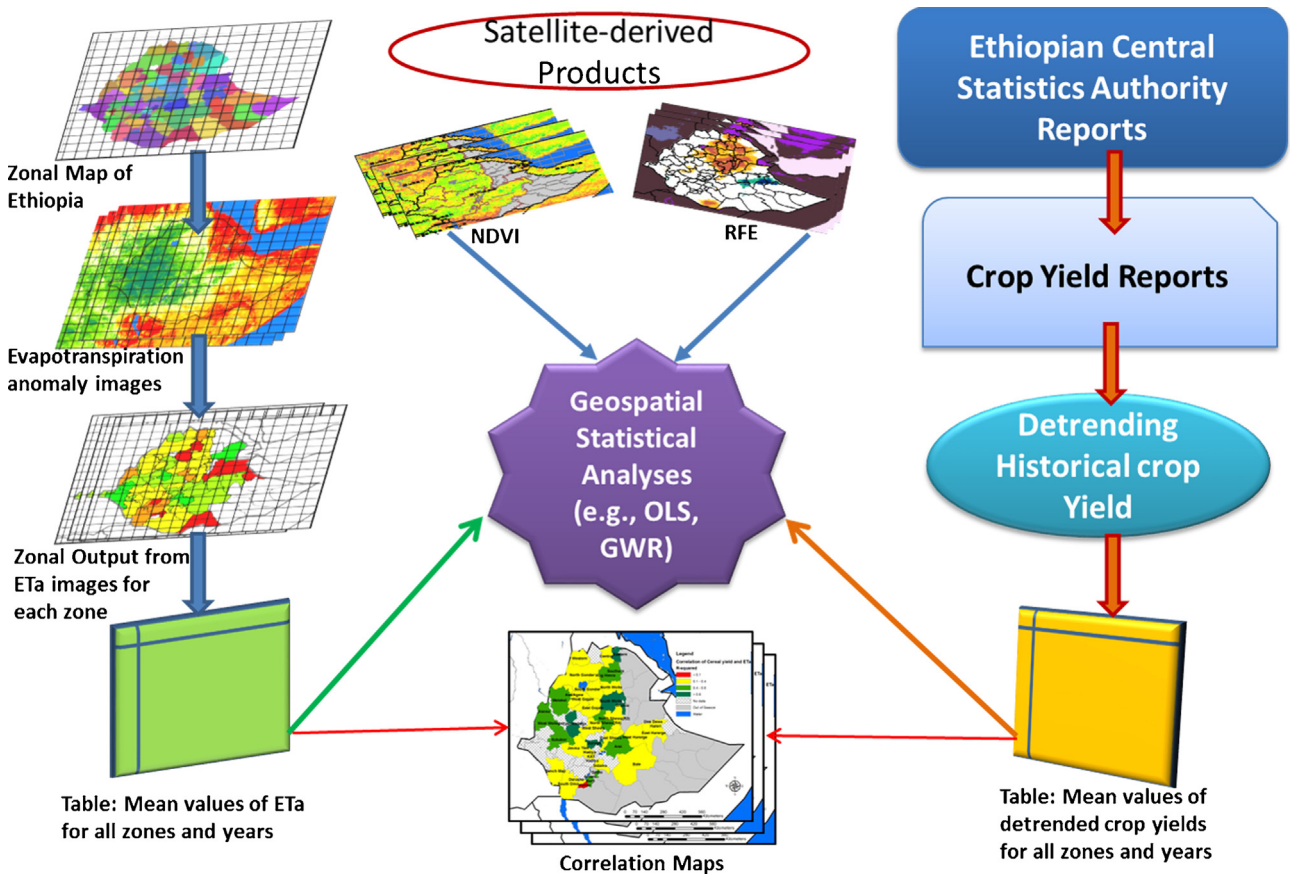

Fig. 3. A process to evaluate satellite-derived evapotranspiration anomaly using RFE, NDVI, and crop yield data: extracting ETa, RFE, and NDVI spatio-temporal data for cropping zones, detrending crop yield, building a database, conducting exploratory statistical analyses, and generating correlation maps.

1998). The OLS has the effect of producing average or global parameter estimates, which are assumed to apply equally over the whole region under analysis (Fotheringham et al., 2002). In other words, the relationships being measured are assumed to be stationary over space. Thus, the OLS (Eq. (6)) was used to identify a global linear relationship between ETa, RFE, NDVI, and crop yield.

$$y_{OLS} = a_0 + \sum_k a_k x_{ik} + \epsilon_i \quad (6)$$

where y_{OLS} is the dependent variable (e.g., global estimated average yield), a_o is the intercept, x_{ik} is the explanatory variables (e.g., average ETa value for given zone), a_k is the coefficient for the explanatory variable, and ϵ_i is the error. All observed data are assumed to be independent and normally distributed.

Extending the OLS to spatial context ("non-stationarity"), GWR was computed using Eq. (7). The GWR is one of several spatial regression techniques that provide a local model for estimating average yield (Wheeler and Tiefelsdorf, 2005; Schabenberger and Gotway, 2005; Fotheringham et al., 2002).

$$y_{GWR} = a_{0i} + \sum_k a_{ik} x_{ik} + \epsilon_i \quad (7)$$

where y_{GWR} is the dependent variable (e.g., estimated average yield), a_{0i} is the intercept at coordinates of the ith point in space, $a_{ik}x_{ik}$ is the local regression coefficient for the kth explanatory variable (e.g., average ETa value for a given zone) at location of the ith point in space, and ϵ_i is the error at location i, which may follow an independent normal distribution with zero mean and homogeneous variance (Wheeler and Tiefelsdorf, 2005). GWR builds a local regression equation for each feature in the dataset. In contrast to the global model (OLS), the regression coefficients in GWR are allowed to vary from location to location. Thus, GWR helps provide a continuous surface of parameter values taken at certain points to denote the spatial variability of the surface. Thus, GWR is assumed to provide powerful and reliable statistics for estimating linear relationships between ETa, NDVI, and crop yield for each year.

2.9. Developing an ETa evaluation process

Fig. 3 shows a process developed to evaluate satellite-derived evapotranspiration anomaly using RFE, NDVI, and crop yield data. The process includes (i) extracting ETa, RFE, and NDVI spatio-temporal historical data (2000-2013) for all selected crop zones in Ethiopia using GIS tools (e.g., in this study, zonal statistical means for each zone and for all years were extracted using ArcGIS software's geostatistical analysis tools), (ii) generating statistical tables (building a database) that include seasonal mean values of ETa, percent average of RFE, and seasonal mean of NDVI for all zones and years, (iii) downloading crop yield data from CSA, (iv) checking a trend in historical crop yield data and detrending, (v) generating a table (building a database) that includes detrended spatial and temporal crop yield data for each zone of Ethiopia, (vi) applying exploratory geospatial statistical analyses on ETa, RFE, NDVI, and crop yield data, and (vii) generating correlation maps and analyzing the results.

3. Results and discussions

3.1. Comparison of seasonal ETa and RFE

The percent average seasonal precipitation estimates (RFE) for the selected cropping zones of Ethiopia in Kiremt season were

compared with the seasonal ETa anomaly for each zone in Ethiopia. The results indicate very strong agreement ($R^2 > 0.99$) between the ETa anomaly and seasonal RFE anomaly for all crop growing zones in Ethiopia. This finding is interesting because the sensors and methods used to estimate the precipitation (RFE) and ETa are significantly different, as described in Sections 2.4 and 2.6 above.

Geospatial statistical analysis has been conducted to identify the temporal and spatial relationships of ETa and RFE. Table 1 summarizes the spatial correlation of the ETa and RFE in each year. In this analysis, both ETa and RFE products were extracted for only crop areas in each zone for each year. Then, the yearly spatial correlations of all selected zones between the seasonal ETa and seasonal percent average of RFE were analyzed.

The OLS spatio-temporal analysis of the relationship and comparison between seasonal ETa and RFE from 2000 to 2013 is also summarized in Table 1. Based on ETa and RFE historical time-series data, the OLS (global model) analysis showed strong correlation (R^2), ranging from 0.9983 to 0.9999. This strong correlation indicates that more than 99% of the variability of seasonal ETa can be explained using the seasonal average of RFE. In Table 1, the "Coefficient" represents the strength and type of relationship between RFE and ETa. The AICc in the RFE as an independent variable was statistically significant at p-value less than 0.01 for all 14 years. Thus, based on the 14 years of historical records, the results showed that there is statistically significant correlation between seasonal ETa and seasonal percent average of RFE in all 14 years.

Fig. 4 shows the spatial distribution of the historical time series (temporal) correlations between seasonal ETa and RFE. In this analysis, the historical records of seasonal ETa and RFE data are correlated for each cropping zone separately and then put together for all zones to produce the correlation map. This map shows the spatial distribution and patterns of the historical time series correlation. As indicated in Fig. 4, except for few zones (i.e., Dire Dawa, Harari, and Gedio), the R^2 between ETa and RFE is greater than 0.9977 for most cropping zones of Ethiopia. Fig. 4 also shows that, there is a relatively stronger correlation between the seasonal ETa and RFE over the northern regions as compared to the southern and southwestern zones of Ethiopia.

3.2. Comparison of the seasonal ETa and seasonal average of the NDVI

To identify the spatio-temporal relationships and assess their correspondence, a comparison of seasonal average NDVI data with the seasonal ETa anomaly was done in this study. Table 2 summarizes the OLS and GWR analysis between seasonal ETa and percent average of seasonal NDVI for all zones included in the study. In this geospatial analysis, the time series historical ETa and NDVI data were extracted for each year across all the cropping zones, and spatial correlations (for each year) between the seasonal ETa and seasonal percent average of NDVI were calculated. The results indicate that for the intercepts of these models, 2001, 2006, 2007, 2010–2013 were found to be statistically significant at p-value < 0.01. The OLS R^2 values ranged from 0.02 in 2011 to 0.7 in 2008 (Table 2). Because OLS develops a global model (one equation applicable for all zones), the GWR that considers local variability within a general model was applied. Subsequently, the R^2 values have generally improved using GWR. Thus, the R^2 using GWR ranged from about 0.4 in 2009 to 0.7 in 2013 (Table 2), showing improvements in all years except 2008.

In addition to the spatio-temporal (yearly) correlation, a correlation analysis was done for each individual cropping zone based on its historical time series records. The results of this analysis are shown in Table 3.

Table 3 shows that relatively higher correlations ($R^2 > 0.4$) were observed between ETa anomaly and NDVI for eleven zones, including Konso, West Harerge, Burji, Eastern Tigray, Arsi, and Bench Maji. Generally, the correlation between seasonal ETa and NDVI was not

Table 1
Summary of OLS results – model variable and spatial correlation (R^2) for ETa and RFE.

Summary of OLS results – model variable and spatio-temporal correlation for seasonal ETa and RFE							
Year	Variable	Coefficient	StdError	t_Statistics	Probability	AICc[a]	R^2
2000	Intercept	0.8615	0.1843	4.6739	0.000035*	−63.90	0.9999
	Percent avg_ RFE	0.9917	0.0019	534.8666	0.000000*		
2001	Intercept	0.0849	0.3846	0.2208	0.826407	−69.06	0.9994
	Percent avg_ RFE	0.9994	0.0038	264.0694	0.000000*		
2002	Intercept	−0.2605	0.3357	−0.7761	0.442346	−16.17	0.9994
	Percent avg_ RFE	1.0025	0.0038	261.0758	0.000000*		
2003	Intercept	0.3222	0.3328	0.9680	0.338987	−69.52	0.9995
	Percent avg_ RFE	0.9967	0.0034	293.1553	0.000000*		
2004	Intercept	0.3592	0.5000	0.7184	0.476765	−18.29	0.9988
	Percent avg_ RFE	0.9961	0.0055	182.4551	0.000000*		
2005	Intercept	0.4048	0.2631	1.5387	0.131943	−90.83	0.9998
	Percent avg_ RFE	0.9959	0.0025	396.3453	0.000000*		
2006	Intercept	1.3366	0.6899	1.9374	0.059958	−67.88	0.9983
	Percent avg_ RFE	0.9871	0.0066	149.9917	0.000000*		
2007	Intercept	0.8000	0.3376	2.3696	0.022855	−45.42	0.9996
	Percent avg_ RFE	0.9922	0.0032	314.2714	0.000000*		
2008	Intercept	−0.0092	0.2256	−0.0407	0.96777	−93.20	0.9998
	Percent avg_ RFE	1.0002	0.0022	456.7065	0.000000*		
2009	Intercept	−0.0077	0.2866	−0.0269	0.978646	−62.82	0.9996
	Percent avg_ RFE	1.0000	0.0033	302.7206	0.000000*		
2010	Intercept	−1.2744	0.7743	−1.6458	0.10784	−18.32	0.9980
	Percent avg_ RFE	1.0122	0.0073	138.0861	0.000000*		
2011	Intercept	−0.7032	0.6070	−1.1585	0.253719	−46.10	0.9986
	Percent avg_ RFE	1.0071	0.0060	167.739	0.000000*		
2012	Intercept	0.3891	0.5370	0.7245	0.473074	−8.77	0.9989
	Percent avg_ RFE	0.9961	0.0053	187.4132	0.000000*		
2013	Intercept	−0.5713	0.5693	−1.0035	0.321827	+1.00	0.9988
	Percent avg_ RFE	1.0056	0.0054	185.1616	0.000000*		

* An asterisk next to a number indicates a statistically significant p-value ($p < 0.01$). Number of observations (zones) = 41.
[a] The AICc (akaike's information criterion second order correction for small sample sizes) is a relative measure of performance used to compare models; the smaller AICc indicates the better the model for that specific year.

Table 2
Summary of OLS and GWR results between seasonal ETa and seasonal NDVI.

Summary of OLS and GWR results – model variables and spatio-temporal correlation for ETa and NDVI								
Year	Variable	Coefficient	StdError	*t*_Statistics	Probability	AICc	OLS R^2	GWR R^2
2001	Intercept	58.1105	15.3745	3.77967	0.00057*	225.7	0.260	0.580
	Seasonal_NDVI	0.41987	0.1477	2.84261	0.007328*			
2002	Intercept	1.22295	24.82293	0.04927	0.96098	281.5	0.188	0.632
	Seasonal_NDVI	0.85977	0.24869	3.45718	0.001418*			
2003	Intercept	15.94791	14.24514	1.11953	0.270327	238.0	0.357	0.603
	Seasonal_NDVI	0.81258	0.14218	5.71524	0.000002*			
2004	Intercept	10.22318	10.22838	0.99949	0.324228	238.6	0.385	0.570
	Seasonal_NDVI	0.81313	0.10129	8.02788	0.000000*			
2005	Intercept	10.34573	20.02664	−0.5166	0.608595	233.5	0.324	0.501
	Seasonal_NDVI	0.47635	0.19593	5.72259	0.000002*			
2006	Intercept	58.88729	15.78812	3.72985	0.000657*	182.8	0.218	0.475
	Seasonal_NDVI	0.44999	0.15425	2.91728	0.006049*			
2007	Intercept	28.68657	12.44457	2.30515	0.027034*	266.6	0.204	0.498
	Seasonal_NDVI	0.7468	0.12036	6.20468	0.000000*			
2008	Intercept	9.18889	7.63577	1.2034	0.236675	208.5	0.707	0.597
	Seasonal_NDVI	0.94898	0.07704	12.31844	0.000000*			
2009	Intercept	19.58183	10.67885	1.8337	0.074976	245.9	0.207	0.431
	Seasonal_NDVI	0.71844	0.1132	6.34652	0.000000*			
2010	Intercept	48.4683	12.03251	4.02811	0.000277*	121.2	0.297	0.450
	Seasonal_NDVI	0.56502	0.11978	4.71724	0.000035*			
2011	Intercept	82.97451	21.85443	3.79669	0.000543*	222.9	0.022	0.632
	Seasonal_NDVI	0.18119	0.2207	0.82097	0.417065			
2012	Intercept	24.98832	11.5631	2.16104	0.037423*	250.8	0.377	0.533
	Seasonal_NDVI	0.76843	0.11838	6.49139	0.000000*			
2013	Intercept	42.04244	19.17159	2.19296	0.034856*	239.2	0.193	0.688
	Seasonal_NDVI	0.64434	0.19701	3.27057	0.002369*			

* An asterisk next to a number indicates a statistically significant *p*-value ($p < 0.01$). Number of observations (zones) = 38.

Table 3
Summary of the historical time series correlation between ETa and NDVI for each individual crop zone in Ethiopia.

Correlation (R^2) between ETa and NDVI for individual crop zone											
$R^2 > 0.4$				$0.2 < R^2 < 0.4$				$R^2 < 0.2$			
Zone name	R^2	Total zone area[a] (km^2)	Crop area[†] (km^2)	Zone name	R^2	Total zone area[†] (km^2)	Crop area[a] (km^2)	Zone name	R^2	Total zone area[†] (km^2)	Crop area[a] (km^2)
Konso	0.84	2274	2046	Gedio	0.39	1352	1217	North Shewa(R4)	0.18	11,531	1153
West Harerge	0.67	16,523	6348	Asosa	0.38	14,166	6972	Central Tigray	0.15	22,134	19,885
Burji	0.63	1128	1016	Amaro	0.37	1422	1280	South Gonder	0.13	14,095	7625
Eastern Tigray	0.52	13,269	6782	Oromia	0.36	3470	2207	Dire Dawa	0.12	1559	156
Arsi	0.51	19,825	5550	Southern Tigray	0.35	18,670	8388	North Wollo	0.11	12,173	5306
Bench Maji	0.50	19,252	12,451	Bale	0.32	43,691	12,675	West Wellega	0.06	12,745	8502
Metekel	0.47	25,688	12,195	North Gonder	0.30	45,945	19,111	Yem	0.04	648	583
Western Tigray	0.44	12,323	6662	Wag Himra	0.24	9039	3367	Hareri	0.04	334	301
East Harerge	0.43	18,240	6230	North Shewa(R3)	0.23	15,936	15,299	South Wollo	0.04	17,067	12,967
West Gojam	0.40	13,312	12,110	East Gojam	0.22	14,004	11,798	Jimma	0.03	18,076	16,268
Awi/Agew	0.40	9148	6285	East Wellega	0.22	13,830	13,465	Gurage	0.01	5893	1879
				West Shewa	0.21	14,789	3374	Hadiya	0.00	3593	3234
								Ilubabor	0.00	16,517	15,734
								KAT	0.00	1356	1220
								Sidama	0.00	6538	5884

[a] The total area of the corresponding zone (in square km) is based on the GeoHive (2014) data. The crop area is calculated using the global land cover map (GlobCover LC v2). Number of observations (years) = 12.

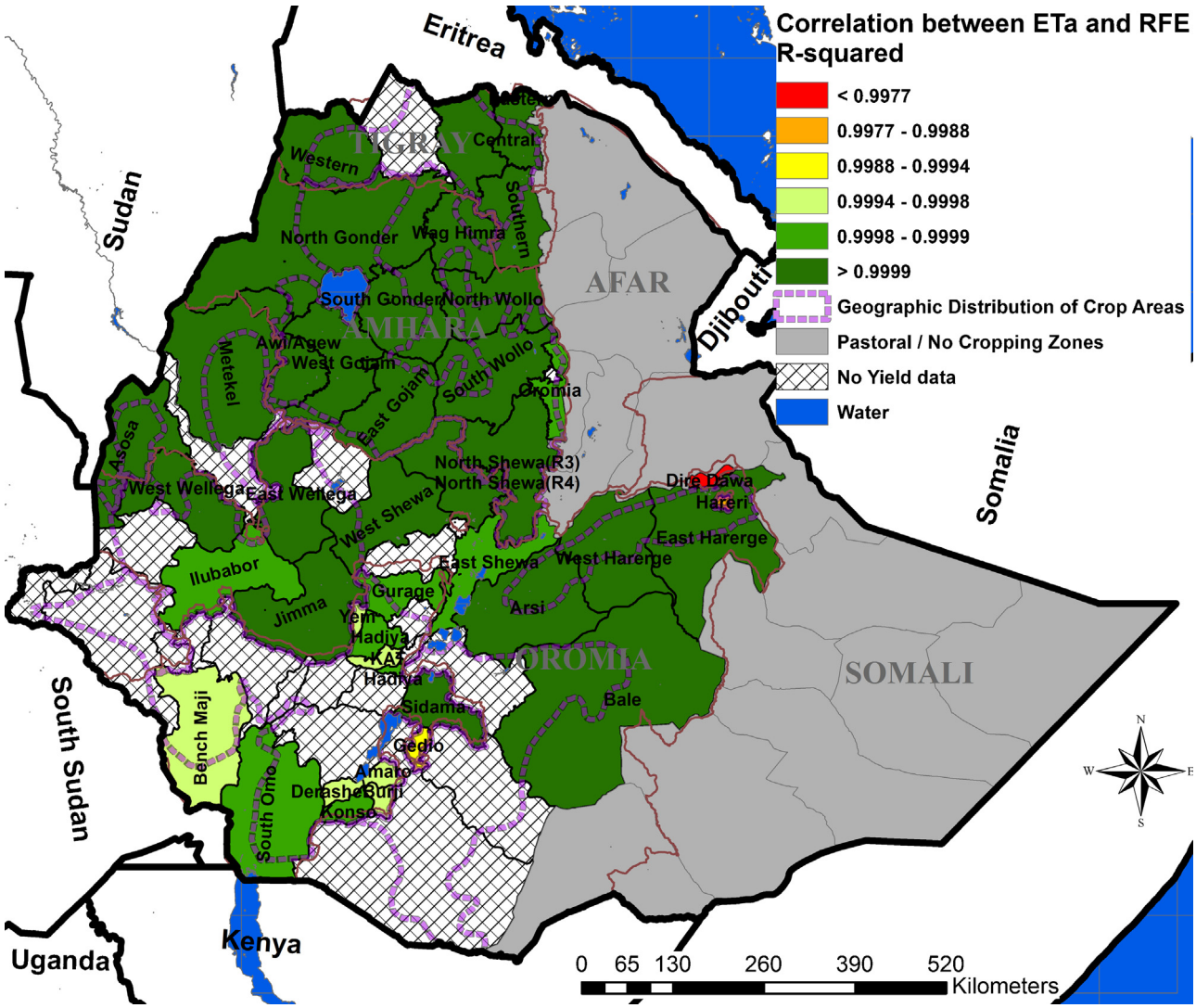

Fig. 4. Spatial distribution of the historical time series correlations between ETa and RFE for all crop zones in Ethiopia.

strong in some parts of the cropping zones of Ethiopia. Eighteen out of thirty-eight zones (47%) had R^2 greater than 0.3. Only eighteen (29%) of the selected cropping zones had relatively higher correlation (i.e., $R^2 > 0.4$). Note that three zones in the southern rift valley (Derashie, East Shewa, and South Omo) were removed from this analysis because of poor data quality (unrealistically high or low percent average, $> \pm 500\%$) in the original NDVI values. Poor data quality could be the result of cloud contamination or other sources of errors such as high variability of the NDVI response of the less vegetated surface across the southern rift valley and the southern low lands. Thus, only 38 (out of 41) zones were used. However, except for data analysis that involves NDVI, those three zones (i.e., Derashie, East Shewa, and South Omo) were used in all other analyses. Fig. 5 shows the spatial distribution of the correlations between the ETa and NDVI. Generally, the eastern highlands of Ethiopia and the western zones had relatively strong correlation (i.e., greater than $R^2 > 0.4$). The southwestern, central, and northern highlands show very low correlation. By contrast, the ETa show higher correlation with RFE in these zones, where NDVI is showing low correlation with ETa. Since the NDVI data are also showing very low correlation with the RFE in these zones, it is possible that the NDVI could have poor performance in these areas due to high cloud coverage during Kiremt season, which may affect the NDVI values. Several factors could result in weak correlations, such as the methods used in the models to estimate the vegetation condition and the different climate parameters that are observed in different wavelengths of the sensors. These factors may have different influences from place to place, affecting the outcome of the relationships. Further investigation is needed to identify the possible causes and generalize the relationships.

3.3. *Spatial and temporal correlations of ETa and cereal yield data*

Cereals are the core of Ethiopia's agriculture and food economy, accounting for about three-quarters of total area cultivated and 29% of agricultural gross domestic product (GDP) in 2005/06 (Taffesse et al., 2011). In this study, cereals comprise mainly the five major crops: teff (a tiny grain known as lovegrass, with a scientific name Eragrostis E. Tef, is an important food grain in Ethiopia), corn, barely, sorghum, and wheat.

The analyses of the cereals yield data in Ethiopia showed a gradual increase in annual production, implying an upward trend in time. This upward increase in yield could be due to improved farm management, such as use of fertilizer, pesticide applications, and improved farming systems through agricultural extension. Thus, in order to identify a meaningful relationship between the crop yield and the ETa, this trend was removed (detrended). Fig. 6 shows an example of detrending for Eastern Tigray zone. In this figure, the

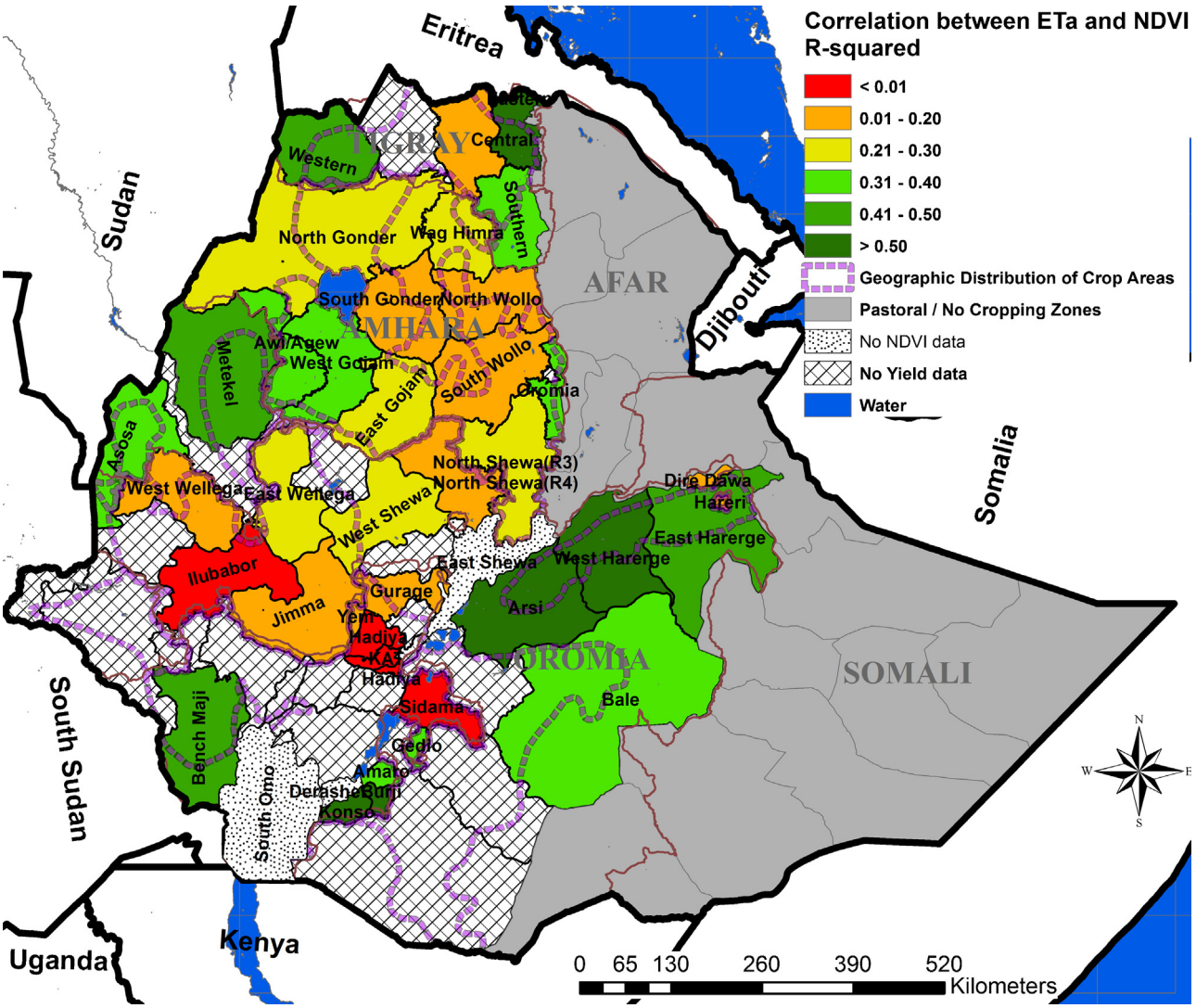

Fig. 5. Spatial distribution of the historical time series correlations between ETa and NDVI for all crop zones in Ethiopia.

linear equation of the trend, the trend line, and detrended values are shown for Eastern Tigray zone. A similar technique was applied to detrend the crop yield for all cropping zones.

Generally, the cereal yield data vary both temporally and spatially. After generating the detrended cereal yield values for all cropping zones, the spatial and temporal relationships between the ETa and detrended crop yield were explored using global regression (OLS). Table 4 summarizes the OLS analyses that were tested to help in predicting crop yield using ETa.

The results showed that OLS models have weak relationships (R^2 < 0.2) on a year-to-year basis where all cropping zones are taken together (Table 4). This finding indicates that a one-size-fits-all model (using a global model) should not be applied to all zones collectively. Because of the weak spatial correlation of OLS and GWR that use all zones collectively, each zone was evaluated separately using historical time series records to identify the relationship of seasonal ETa. Table 5 summarizes the correlation (R^2) between ETa and cereal yield for each crop zone in Ethiopia. Interestingly, the results showed some zones have a stronger relationship with ETa separately than the general spatial models that include all crop zones together.

As shown in Table 5, correlating ETa and detrended cereals for each zone for all years (historical time series) produced relatively higher R^2 values. The results of this analysis indicate that 26 out of 41 crop zones in Ethiopia had greater than 0.5 R^2 values. This is about 63% (179,363 km^2) of the area that is classified as crop land in Ethiopia, based on the global land cover map (GlobCover LC v2). Furthermore, the R^2 values were between 0.5 and 0.6, between 0.6 and 0.7, and more than 0.7 for about 23% (66,416 km^2), 19% (56,326 km^2), and 19% (56,620 km^2) of the cropping areas in Ethiopia, respectively. Only about 13% of the crop zones (37,546 km^2) had less than 0.3 R^2 values.

The highest R^2 (0.82) was observed for Eastern Tigray zone in the northern region of Ethiopia. The lowest R^2 was 0.01 for South Omo zone in the Southern Nations, Nationalities, and Peoples' region (SNNP) of Ethiopia. Generally, the northern and central regions of Ethiopia showed better correlation (high R^2 values) than the southern lowlands. One of the possible explanations for this difference in R^2 could be the contrasting elevation differences between the mountainous regions and lowlands. The assumption here was that the ETa model may be influenced by heterogeneity of the zones in elevation (Senay et al., 2011). Based on this assumption, the influences of elevation on the correlation coefficient of the relationships between ETa and crop yield data were analyzed. The result of this analysis showed that the elevation data (using Digital Elevation Model) can explain only about 7% of the variability in the R^2 between ETa and crop yield data. Thus, further investigation is needed to better explain the higher and lower R^2

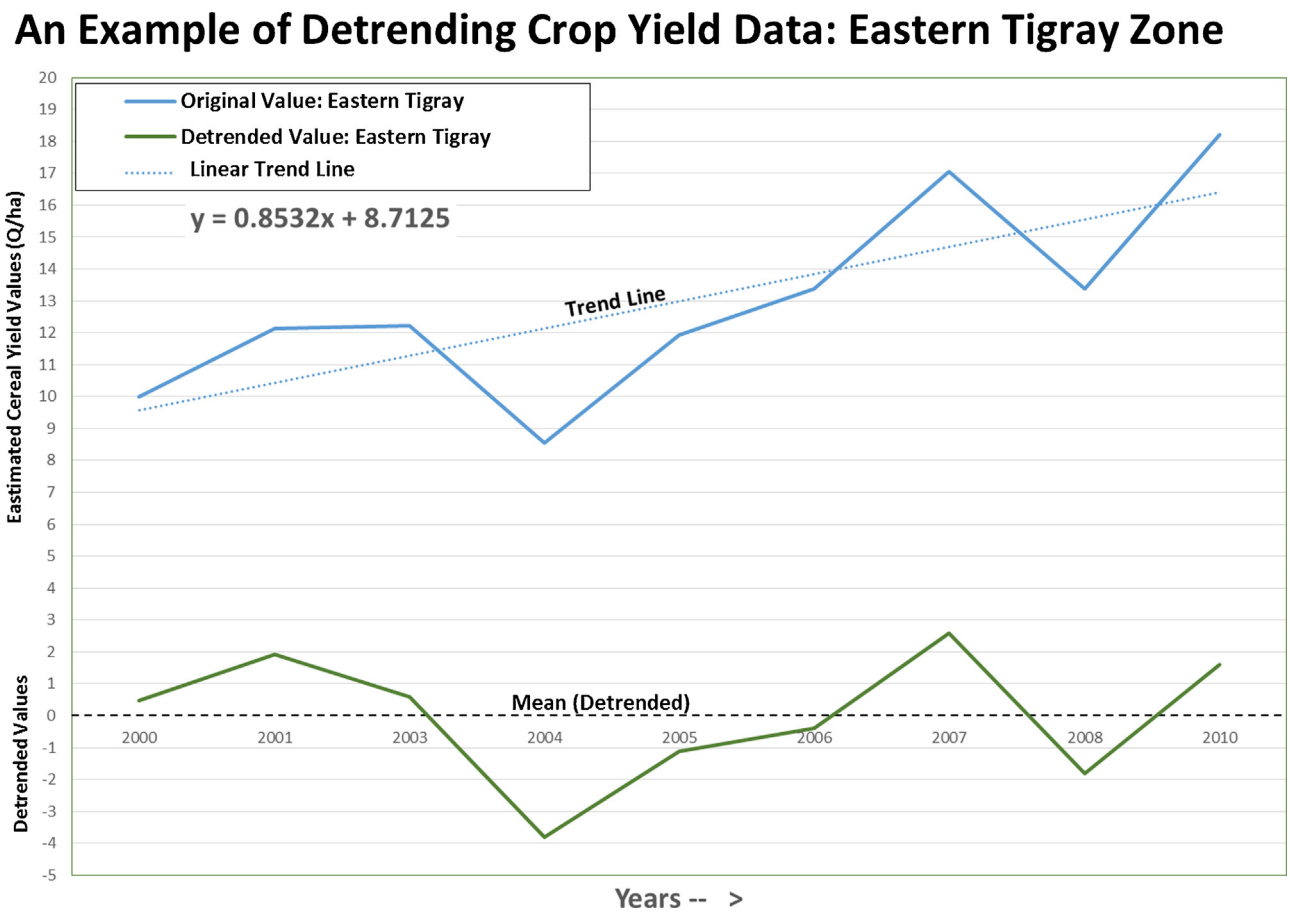

Fig. 6. An example of detrending technique using Eastern Tigray zone historical data. The average or normal value is zero for the detrended crop yields. The positive values (above the trend line) show more productive years and the negative values show lower production as compared to the expected mean. This detrending was done for all cropping zones in Ethiopia.

values across the northern mountains and the southern lowlands, respectively.

Fig. 7 shows the spatial distribution of the R^2 values for the detrended cereal crop yield. Generally, the spatial distribution showed that medium to high correlations between ETa and cereal yield were found across the zones that grow cereal during Kiremt season in Ethiopia. The lowest correlated areas were across the south and southwest, and the southern parts of the eastern highlands, including East Hararghe, Bale, Konso, South Omo and Bench Maji. This pattern resembles the seasonal northward shift of

Table 4
Summary of OLS results – model variable and spatial correlation for ETa and detrended cereals yield for each year.

Summary of OLS – model variable and spatio-temporal correlation for seasonal ETa and detrended cereals							
Year	Variable	Coefficient	StdError	*t*_Statistics	Probability	AICc	OLS R^2
2000	Intercept	5.9884	2.8243	2.1203	0.0409	128.05	0.1056
	Seasonal_ETa	−0.0580	0.0281	−2.0617	0.0465		
2001	Intercept	5.5195	4.9422	1.1168	0.2715	120.11	0.0191
	Seasonal_ETa	−0.0407	0.0485	−0.8391	0.4069		
2003	Intercept	−2.2209	4.6389	−0.4787	0.6350	125.93	0.0031
	Seasonal_ETa	0.0159	0.0476	0.3347	0.7398		
2004	Intercept	−12.9523	8.7418	−1.4817	0.1471	176.22	0.0492
	Seasonal_ETa	0.1293	0.0947	1.3663	0.1803		
2005	Intercept	0.8320	5.6778	0.1465	0.8843	143.88	0.0019
	Seasonal_ETa	−0.0141	0.0544	−0.2593	0.7969		
2006	Intercept	−4.7296	12.1915	−0.3879	0.7003	151.98	0.0036
	Seasonal_ETa	0.0419	0.1162	0.3612	0.7201		
2007	Intercept	−8.9355	7.2101	−1.2393	0.2233	170.46	0.0445
	Seasonal_ETa	0.0882	0.0681	1.2959	0.2033		
2008	Intercept	−4.4854	4.8643	−0.9221	0.3626	143.08	0.0252
	Seasonal_ETa	0.0455	0.0471	0.9663	0.3404		
2010	Intercept	−2.6279	5.6050	−0.4689	0.6420	126.87	0.0101
	Seasonal_ETa	0.0323	0.0533	0.6073	0.5474		

Number of observations (zones) = 38. The crop yield data for 2002 and 2009 are missing (i.e., excluded from this analysis).

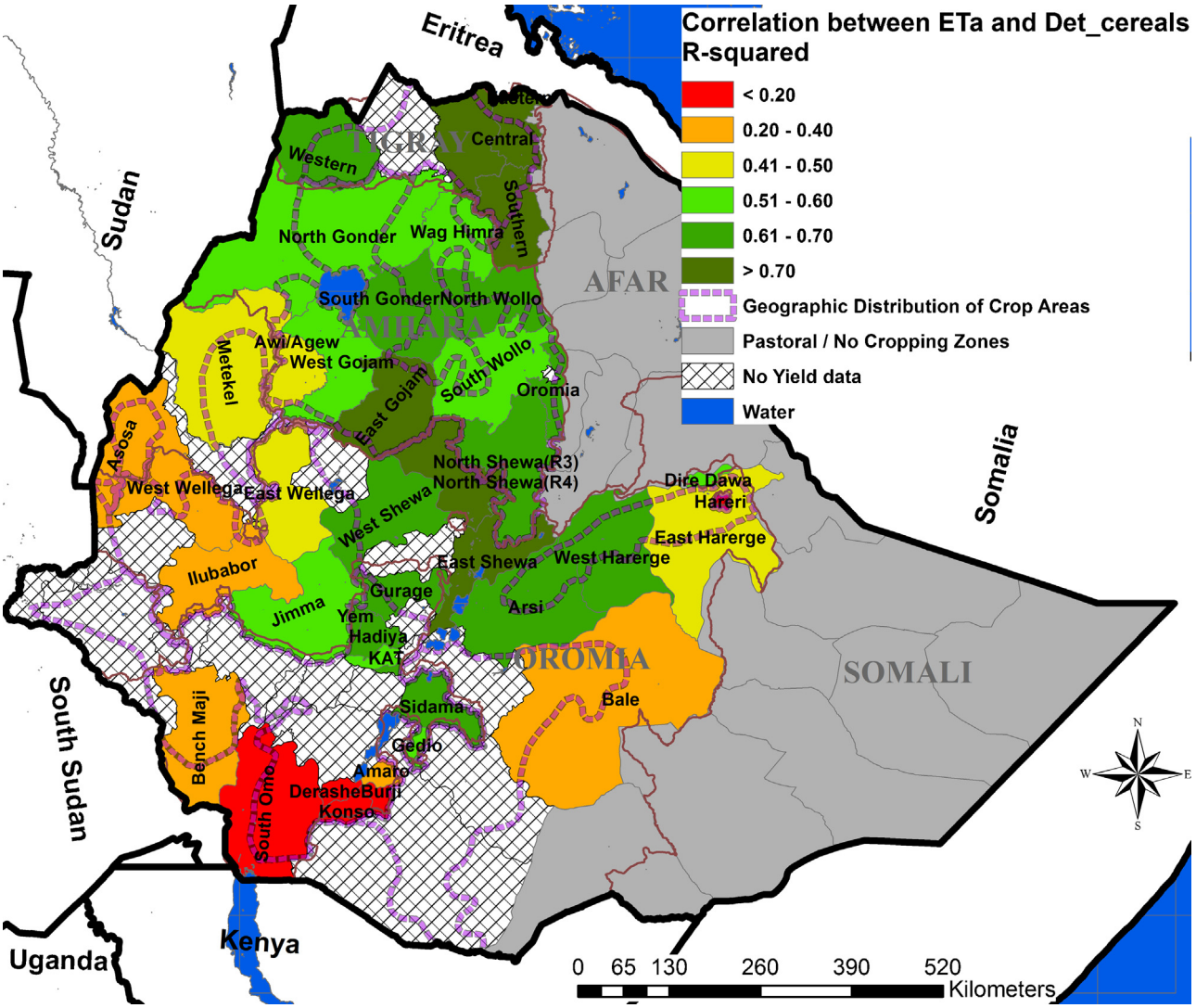

Fig. 7. Spatial distribution of the historical time series correlations between ETa and de-trended cereal yield for all crop zones in Ethiopia.

the Kiremt rain belt (i.e., the northward shift of the Inter-Tropical Convergence Zone, ITCZ). The relatively less rainy condition in the southern part of Ethiopia during Kiremt season and its impact on vegetation condition may have an influence on the relationship between the ETa and crop yield.

4. Future research

The seasonal ETa model and products showed relatively good correlation to predict the potential yield in the main cereal growing zones. However, several factors and possible errors could influence the results of this study. One of the main factors is the data quality of ETa, RFE, and crop yields that include poor (realistically inaccurate) and missing data, and biases/errors in the methods of estimating the variables. The ETa model has an inherent inaccuracy in estimating the actual evapotranspiration. For example, significant error may result because of a bias in the use of a constant pre-defined differential temperature between the hot/dry and cold/wet boundary conditions for each pixel (Senay et al., 2013). The spatial averaging of the NDVI and RFE over a large area (e.g., zonal or regional level) could also introduce significant errors. Obviously, the remote sensing products (ETa, NDVI, and RFE) need to be thoroughly evaluated using ground observations. The only "ground observation" that was used in this study was the CSA estimate of crop yield data. Even though an attempt has been made to estimate crop yield with better accuracy in Ethiopia, the analyses in this study showed that cereal yield estimates for a few zones were significantly different from the neighboring zones. On the other hand, it is recognized that farming practices, such as land preparation, timing of seeding, and crop and water management, have a substantial effect on yields of cereal and other crops (Pretty and Hine, 2001; World Bank, 2007). This is particularly important in Ethiopia, where farming practices vary greatly across ethnic and agroecological zones (Tilahun et al., 2011). Future studies may incorporate these factors to refine the relationship and applicability of ETa products in estimating the crop yields.

Furthermore, unavailability of crop yield data for some zones in the southern and southwestern regions limited the analyses of the study and could introduce errors in the results. In addition, the crop yield data were for eleven years only, and two years (out of eleven) are missing for all crop zones in the country. Specifically, the missing years could have a significant impact on detrending the crop yield. With long records of historical crop yield data, the results of this study are expected to improve significantly. Moreover, since the zonal administrative level has a coarse spatial resolution (about 15,000 km^2), the aggregated crop yields and ETa data for each zone may not show the local (e.g., district) variability of crop yield and ETa data. Optimally higher spatial resolution of crop yield data

Table 5
Summary of the historical time series correlation between ETa and detrended cereal yield for each individual crop zone in Ethiopia.

Correlation (R^2) between ETa and detrended cereal yield for individual crop zone												
$R^2 > 0.7$			$0.6 < R^2 < 0.7$			$0.5 < R^2 < 0.6$			$0.3 < R^2 < 0.5$			$R^2 < 0.3$		
Zone name	R^2	Area[a] (Km^2)	Zone name	R^2	Area[a] (Km^2)	Zone name	R^2	Area[a] (Km^2)	Zone name	R^2	Area[a] (Km^2)	Zone name	R^2	Area[a] (Km^2)
Eastern Tigray	0.82	6782 (13,269)	Sidama	0.69	5884 (6538)	South Wollo	0.59	12,967 (17,067)	East Wellega	0.49	13,465 (13,830)	West Wellega	0.29	8502 (12,745)
Southern Tigray	0.81	8388 (18,670)	Western Tigray	0.69	6662 (12,323)	KAT	0.58	1220 (1356)	East Harerge	0.48	6230 (18,240)	Bale	0.25	12,675 (3691)
North Shewa(R4)	0.78	1153 (11,531)	North Wollo	0.69	5306 (12,173)	West Gojam	0.58	12,110 (13,312)	Awi/ Agew	0.46	6285 (9148)	Hareri	0.17	301 (334)
East Shewa	0.76	989 (9893)	Gurage	0.68	1879 (5893)	Gedio	0.54	1217 (1352)	Metekel	0.43	12,195 (25,688)	Derashe	0.16	1339 (1487)
Central Tigray	0.75	19,885 (22,134)	West Shewa	0.68	3374 (14,789)	North Gonder	0.54	19,111 (45,945)	Asosa	0.4	6972 (14,166)	Konso	0.04	2046 (2274)
East Gojam	0.75	11,798 (14,004)	Yem	0.68	583 (648)	Wag Himra	0.54	3367 (9039)	Ilubabor	0.39	15,734 (16,517)	Burji	0.02	1016 (1128)
South Gonder	0.70	7625 (14,095)	North Shewa(R3)	0.67	15,299 (15,936)	Jimma	0.53	16,268 (18,076)	Bench Maji	0.38	12,451 (19,252)	South Omo	0.01	11,668 (21,056)
			Arsi	0.64	5550 (19,825)	Dire Dawa	0.51	156 (1559)	Amaro	0.33	1280 (1422)			
			Hadiya	0.63	3234 (3593)									
			Oromia (zone)	0.62	2207 (3470)									
			West Harerge	0.61	6348 (16,523)									

[a] The area shown in the table is crop area based on the global land cover map (GlobCover LC v2). The figures in brackets are the total surface area of the corresponding zone in square km. Number of observations (years) = 10.

(such as a district locally known as "Woreda" level, which is the lowest administrative boundary and highest spatial resolution) could better represent the crop area and may reduce such errors. Thus, using district administrative level crop estimates (even though the data are not yet available to the general public) may improve the spatial resolution to study local variability of the crop yield and its correlation with ETa.

4. Summary and conclusions

Satellite-derived vegetation and drought monitoring tools including ETa anomaly, NDVI, and merged (satellite and ground observation) RFE products are currently used by USGS FEWS NET for agricultural drought monitoring and food security status assessment in Africa. These products are expected to capture the weather variability and its impact on crop yield. In this study, a process to evaluate and assess the potential use of satellite-derived evapotranspiration anomaly using crop yield data was developed. This process includes exploring the variables (e.g., ETa and crop yield) using geospatial exploratory and statistical techniques.

CSA yield estimates for Ethiopia's main cereal crops (i.e., teff, sorghum, corn/maize, barley, and wheat) during the long rainy season were used in identifying relationships (correlation) with ETa and evaluating the potential use of the ETa products. Because the crop yield historical time series (2000–2010) data showed an increasing trend regardless of the extreme weather events (possibly due to human intervention), the trend was removed before doing any geospatial statistical analysis between ETa and crop yields. After removing the trend, OLS regression analysis techniques were used to identify the relationships.

The seasonal ETa products were also compared with seasonal percent average NDVI and RFE to identify the spatio-temporal relationships and assess their correspondence for all crop zones in Ethiopia. Interestingly, it was found that there is a strong spatio-temporal correlation (i.e., R^2 greater than 0.9) between ETa and RFE. This finding may indicate the dominance of a strong rainfed hydrologic process in most parts of Ethiopia. Comparatively, the correlation between the seasonal ETa and NDVI was not as strong as expected. The spatial correlation (R^2) between ETa and NDVI for each year ranged from 0.02 to 0.7 and 0.4 to 0.7 using OLS (global model) and GWR (local model), respectively. However, the historical time series (temporal) correlation analyses (between ETa and NDVI) for each individual zones showed 47% of crop zones in Ethiopia had R^2 greater than 0.3.

The results of the spatial regression analyses of ETa and detrended crop yields using OLS also did not show strong yearly temporal relationships for all cropping zones collectively. The R^2 between ETa and detrended crop yield ranged from 0.01 to 0.20 using OLS. Thus, predicting spatial variability with the global models may not be warranted. On the other hand, using historical time series records for each individual zone, it was found that some zones have a stronger relationship with ETa separately. The results of this individual zone correlation analysis (between ETa and detrended cereals yield) showed 26 out of 41 crop zones in Ethiopia had R^2 values greater than 0.5, covering 63% (179,363 km2) of crop land in Ethiopia. Thus, the study indicates a potential use of the ETa products as complementary tools to estimate the cereal yield for some individual crop zones, including northern, northwestern, central, and eastern Ethiopia. These zones are the main crop growing areas in Ethiopia. However, caution should be taken while using the ETa products in estimating crop yields for all zones, especially for southwestern and southern Ethiopia.

Because of the limitation of several vegetation monitoring tools, the use of ETa, NDVI, and RFE for assessing crop production and/or food security seems to be growing. Thus, improved ETa and other

remote sensing products such as NDVI and RFE could help in early assessment of food shortages across crop growing zones of Ethiopia during drought years. Generally, this study showed that ETa maps could be used as a complementary tool to monitor vegetation conditions including crops. Such information is expected to support the early warning system and help in improving agricultural drought monitoring and food security. However, despite substantial advances in improving satellite-based models, extreme caution should be taken in using such satellite-derived products for decision making.

Acknowledgements

This research was supported in part by the USGS grant number G12AP20022. The authors are also very grateful for the financial support provided by NASA grant number NNX14AD30G. The authors wish to thank James Rowland and Bruce Dvorak for their encouragement and unreserved support to conduct this study, Stefanie Bohms for providing satellite-derived data used in the study, and Deborah Wood for her editorial suggestion. Any use of trade, firm, or product names is for descriptive purposes only and does not imply endorsement by the authors or U.S. Government.

Appendix A. Supplementary data

Supplementary data associated with this article can be found, in the online version, at http://dx.doi.org/10.1016/j.jag.2015.03.006.

References

Anderson, M.C., Norman, J.M., Mecikalski, J.R., Otkin, J.P., Kustas, W.P., 2007. A climatological study of evapotranspiration and moisture stress across the continental U.S. based on thermal remote sensing: I. Model formulation. J. Geophy. Res. 112 (D10), 117, http://dx.doi.org/10.1029/2006JD007506.

Allen, R.G., Tasumi, M., Trezza, R., 2007. Satellite-based energy balance for mapping evapotranspiration with internalized calibration (METRIC) – Model. J. Irrig. Drain. Eng. 133, 380–394.

Bastiaanssen, W.G.M., Noordman, H., Pelgrum, G., Thoreson, B.P., Allen, R.G., 2005. SEBAL model with remotely sensed data to improve water resources management under actual field conditions. J. Irrig. Drain. Eng. 131, 85–93.

Bastiaanssen, W.G.M., P. Karimi, L-M. Rebelo, Z., Duan, G.B., Senay, L. Muttuwatte, V. Smakhtin, 2014. Earth Observation-based Assessment of the Water Production and Water Consumption of Nile Basin Agro-Ecosystems. Remote Sensing, 6, 1-x manuscripts; doi:10.3390/rs60x000x (accepted, pending revision).

Brown, J.F., Wardlow, B.D., Tadesse, T., Hayes, M.J., Reed, B.C., 2008. The Vegetation Drought Response Index (VegDRI): a new integrated approach for monitoring drought stress in vegetation. GISci. Remote Sens. 45 (1), 16–46.

CSA, 2014. Annual Agricultural Sample Survey. Addis Ababa, Central Statistical Agency of Ethiopia (CSA). http://www.csa.gov.et/index.php/2013-02-20-13-43-35/2013-02-20-13-45-32/annual-agricultural-sample-survey (accessed 06.14.).

DeBeurs, K.M., Henebry, G.M., 2004. Land surface phenology, climatic variation, and institutional change: analyzing agricultural land cover change in Kazakhstan. Remote Sens. Environ. 89 (4), 497–509.

Dinku, T.P., Block, J., Sharoff, K., Hailemariam, D., Osgood, J., del Corral, R., Cousin, M., 2014. Bridging Critical Gaps in Climate Services and Applications in Africa. Earth Perspectives 1, 15, http://dx.doi.org/10.1186/2194-6434-1-15 (accessed 07.14.) http://www.earth-perspectives.com/content/1/1/15

Dinku, T., Ceccato, P., Grover-Kopec, E., Lemma, M., Connor, S.J.J., Ropelewski, C.F., 2007. Validation of satellite rainfall products over East Africa's complex topography. Int. J. Remote Sens. 28, 1503–1526.

Diro, G.T., Grimes, D.I.F., Black, E.C.L., O'Neill, A., Pardo-Igúzquiza, E., 2008. Evaluation of reanalysis rainfall estimates over Ethiopia using monthly raingauge data. Int. J. Climatol. 29 (1), 67–78.

ESRI, 2014. ArcGIS ArcMap Guide. Environmental Systems Resource Institute (ESRI), Redlands, CA.

European Space Agency, 2008. GlobCover Land Cover v2 2008 database. European Space Agency GlobCover Project, led by MEDIAS-France. http://geoserver.isciences.com:8080/geonetwork/srv/en/metadata.show (accessed 07.14.).

Evangelista, P., Young, N., Burnett, J., 2013. How will climate change spatially affect agriculture production in Ethiopia? Case studies of important cereal crops. Clim. Change 119, 855–873.

FAO, 1999. Production variability and losses. In: Gommes, R. (Ed.), Special: Agroclimatic Concepts. Sustainable Development Department (SD), Food and Agriculture Organization of the United Nations (FAO) (accessed 07.14.) http://www.fao.org/sd/eidirect/agroclim/riskdef.htm

FEWSNET, 2003. Estimating Meher crop production using rainfall in the 'long cycle' region of Ethiopia, June 21, revised October 6, http://reliefweb.int/sites/reliefweb.int/files/resources/9EC256793FA1685C49256DB90003E3DC-fews-eth-06oct2.pdf (accessed 07.14.).

FEWSNET, 2014. Famine Early Warning Systems Network, FEWSNET, http://earlywarning.usgs.gov/fews/ (accessed 07.14.).

Fotheringham, A.S., Brunsdon, C., Charlton, M.E., 2002. Geographically Weighted Regression: The Analysis of Spatially Varying Relationships. Wiley, Chichester, UK.

Fotheringham, A.S., Charlton, M.E., Brunsdon, C., 1998. Geographically weighted regression: a natural evolution of the expansion method for spatial data analysis. Environ. Plann. 30, 1905–1927.

GeoHive, 2014. Global Data, Ethiopia. http://www.geohive.com/cntry/ethiopia.aspx (accessed 07.14.).

Gissila, T., Black, E., Grimes, D., Slingo, J., 2004. Seasonal forecasting of the Ethiopian summer rains. Int. J. Climatol. 24, 1345–1358.

Huffman, G.J., Adler, R.F., Bolvin, D.T., Gu, G., Nelkin, E.J., Bowman, K.P., Hong, Y., Stocker, E.F., Wolf, D.B., 2007. The TRMM multisatellite precipitation analysis (TMPA): quasi-global, multiyear, combined-sensor precipitation estimates at fine scales. J. Hydrometeorol. 8, 38–55.

Jakubauskas, M.E., Peterson, D.L., Kastens, J.H., Legates, D.R., 2002. Time series remote sensing of landscape-vegetation interactions in the southern Great Plains. Photogramm. Eng. Remote Sens. 68, 1021–1030.

Joyce, R.J., Janowiak, J.E., Arkin, P.A., Xie, P., 2004. CMORPH: a method that produces global precipitation estimates from passive microwave and infrared data at high spatial and temporal resolution. J. Hydrometeorol. 5, 487–503.

Kanamitsu, M., 1989. Description of the NMC global data assimilation and forecast system. Weather Forecasting 4, 334–342.

Lloyd, C.D., 2007. Local Models for Spatial Analysis. CRC, Boca Raton.

Malingreau, J.P., 1986. Global vegetation dynamics: satellite observations over Asia. Int. J. Remote Sens. 7, 1121–1146.

MathWorks, 2009. MATLAB Neural Network Toolbox User's Guide. The MathWorks, Inc., Natick, MA.

Meze-Hausken, E., 2004. Contrasting climate variability and meteorological drought with perceived drought and climate change in northern Ethiopia. Clim. Res. 27, 19–31.

Mishra, A.K., Singh, V.P., 2011. Drought modeling–a review. J. Hydrol. 403, 157–175.

Mu, Q., Heinsch, F.A., Zhao, M., Running, S.W., 2007. Development of a global evapotranspiration algorithm based on MODIS and global meteorology data. Remote Sens. Environ. 111, 519–536.

Mu, Q., Zhao, M., Running, S.W., 2011. Improvements to a MODIS global terrestrial evapotranspiration algorithm. Remote Sens. Environ. 115, 1781–1800.

Myneni, R.B., Keeling, C.J., Asrar, G., Nemani, R.R., 1997. Increased plant growth in the northern high latitudes from 1981 to 1991. Nature 386, 695–702.

NOAA, 2014. National Weather Service, Climate Prediction Center: African Rainfall Estimates. http://www.cpc.ncep.noaa.gov/products/fews/rfe.shtml (accessed 07.14.).

Panu, U.S., Sharmat, T.C., 2002. Challenges in drought research: some perspectives and future directions. Hydrol. Sci. J.—des Sci. Hydrol. 47 (S), S19–S30.

Pretty, J., Hine, R., 2001. Reducing food poverty with sustainable agriculture: a summary of new evidence. In: Final Report of the Safe World Research Project. University of Essex, UK.

Reed, B.C., Loveland, T.R., Tieszen, L.L., 1996. An approach for using AVHRR data to monitor U.S. Great Plains grasslands. Geocarto Int. 11 (3), 13–22.

Rojas, O., Vrieling, A., Rembold, F., 2011. Assessing drought probability for agricultural areas in Africa with coarse resolution remote sensing imagery. Remote Sens. Environ. 115, 343–352.

Schabenberger, O., Gotway, C.A., 2005. Statistical Methods for Spatial Data Analysis. Chapman & Hall, London.

Seifu, A., 2004. Rainfall Variation and its Effect on Crop Production in Ethiopia. M. Sc. thesis. School of Graduate Studies, Addis Ababa University, Ethiopia.

Senay, G.B., Budde, M., Verdin, J.P., Melesse, A.M., 2007. A coupled remote sensing and simplified surface energy balance approach to estimate actual evapotranspiration from irrigated fields. Sensors 7, 979–1000.

Senay, G.B., Verdin, J.P., Lietzow, R., Melesse, A.M., 2008. Global daily reference evapotranspiration modeling and evaluation. J. Am. Water Res. Assoc. 44, 969–979.

Senay, G.B., Budde, M.E., Verdin, J.P., 2011. Enhancing the simplified surface energy balance (SSEB) approach for estimating landscape ET: validation with the METRIC model. Agric. Water Manage. 98, 606–618.

Senay, G.B., Bohms, S., Singh, R.K., Gowda, P.H., Velpuri, N.M., Alemu, H., Verdin, J.P., 2013. Operational evapotranspiration mapping using remote sensing and weather datasets: a new parameterization for the SSEB approach. J. Am. Water Res. Assoc. 49 (3), 577–591, http://dx.doi.org/10.1111/jawr.12057.

Swets, D.L., Reed, B.C., Rowland, J.D., Marko, S.E., 1999. A weighted least-squares approach to temporal NDVI smoothing. In: 1999 ASPRS Annual Conference: From Image to Information, Portland, Oregon, May 17–21. Proceedings, American Society for Photogrammetry and Remote Sensing, Bethesda, Maryland.

Tadesse, T., Haile, G., Knutson, C., Wardlow, B.D., 2008. Building integrated drought monitoring and food security systems in sub-Saharan Africa. U.N. Natural Res. Forum 32, 303–316.

Tadesse, T., Wardlow, B.D., Hayes, M.J., Svoboda, M.D., Brown, J.F., 2010. The vegetation condition outlook (VegOut): a new method for predicting vegetation seasonal greenness. GISci. Remote Sens. 47 (1), 25–52.

Tadesse, T., Demisse, G.B., Zaitchik, B., Dinku, T., 2014. Satellite-based hybrid drought monitoring tool for prediction of vegetation condition in Eastern Africa: a case study for Ethiopia. Water Resour. Res. 50, 2176–2190, http://dx.doi.org/10.1002/2013WR014281.

Taffesse, A.S., Dorosh, P., Asrat, S., 2011. Crop production in Ethiopia: regional patterns and trends. In: ESSP II Working Paper 16. International Food Policy Research Institute/Ethiopia Strategy Support Program II, Addis Ababa, Ethiopia.

Tilahun, H., Teklu, E., Michael, M., Fitsum, H., Awulachew, S.B., 2011. Comparative performance of irrigated and rainfed agriculture in Ethiopia. World Appl. Sci. J. 14 (2), 235–244.

Townshend, J.R.G., Justice, C.O., Kalb, V., 1987. Characterization and classification of South American land cover types using satellite data. Int. J. Remote Sens. 8, 1189–1207.

Tucker, C.J., Townshend, J.R.G., Goff, T.E., 1985. African land cover classification using satellite data. Science 9227 (4685), 369–375.

Velpuri, N.M., Senay, G.B., Singh, R.K., Bohms, S., Verdin, J.P., 2013. A comprehensive evaluation of two MODIS evapotranpiration products over the conterminous United States: using point and gridded FLUXNET and water balance ET. Remote Sens. Environ. 139, 35–49.

Vicente-Serrano, S.M., Beguería, S., Eklundh, L., Gimeno, G., Weston, D., Kenawy, A.E., López-Moreno, J.I., Nieto, R., Ayenew, T., Konte, D., Ardö, J., Pegram, G.G.S., 2012. Challenges for drought mitigation in Africa: the potential use of geospatial data and drought information systems. Appl. Geogr. 34, 471–486.

Wheeler, D., Tiefelsdorf, M., 2005. Multicollinearity and correlation among local regression coefficients in geographically weighted regression. J. Geogr. Syst. 7, 161–187.

World Bank, 2007. The perception of and adaptation to climate change in Africa. http://www.thefreelibrary.com/The+perception+of+and+adaptation+to+climate+change+in+Africaa0221761216 (accessed 07.14.).

Wu, Z., Huang, N.E., Long, S.R., Peng, C.K., 2007. On the trend, detrending, and variability of nonlinear and nonstationary time series. Proc. Natl. Acad. Sci. 104 (38), 14889–14894.